GEOLOGY | THE GEOLOGICAL SOCIETY OF AMERICA®

https://doi.org/10.1130/G46965.1

Manuscript received 5 September 2019
Revised manuscript received 17 January 2020
Manuscript accepted 23 January 2020

Published online 18 March 2020

Hematite (U-Th)/He thermochronometry detects asperity flash heating during laboratory earthquakes

Gabriele Calzolari[1], Alexis K. Ault[1], Greg Hirth[2] and Robert G. McDermott[1]
[1]Department of Geosciences, Utah State University, Logan, Utah 84322, USA
[2]Department of Earth, Environmental and Planetary Sciences, Brown University, Providence, Rhode Island 02912, USA

ABSTRACT

Evidence for coseismic temperature rise that induces dynamic weakening is challenging to directly observe and quantify in natural and experimental fault rocks. Hematite (U-Th)/He (hematite He) thermochronometry may serve as a fault-slip thermometer, sensitive to transient high temperatures associated with earthquakes. We test this hypothesis with hematite deformation experiments at seismic slip rates, using a rotary-shear geometry with an annular ring of silicon carbide (SiC) sliding against a specular hematite slab. Hematite is characterized before and after sliding via textural and hematite He analyses to quantify He loss over variable experimental conditions. Experiments yield slip surfaces localized in an ~5–30-µm-thick layer of hematite gouge with <300-µm-diameter fault mirror (FM) zones made of sintered nanoparticles. Hematite He analyses of undeformed starting material are compared with those of FM and gouge run products from high-slip-velocity experiments, showing >71% ± 1% (1σ) and 18% ± 3% He loss, respectively. Documented He loss requires short-duration, high temperatures during slip. The spatial heterogeneity and enhanced He loss from FM zones are consistent with asperity flash heating (AFH). Asperities >200–300 µm in diameter, producing temperatures >900 °C for ~1 ms, can explain observed He loss. Results provide new empirical evidence describing AFH and the role of coseismic temperature rise in FM formation. Hematite He thermochronometry can detect AFH and thus seismicity on natural FMs and other thin slip surfaces in the upper seismogenic zone of Earth's crust.

INTRODUCTION

Earthquakes dissipate most energy as heat (e.g., Kanamori and Riviera, 2006). Temperature rise on thin slip surfaces facilitates fault weakening, rupture propagation, and transformation of mechanical and chemical rock properties that influence subsequent fault slip (e.g., Di Toro et al., 2011; Goldsby and Tullis, 2011). However, documenting coseismic paleotemperatures in exhumed fault rocks is challenging, owing to overprinting thermal, physio-chemical, and deformation processes (Rowe and Griffith, 2015). Thermally activated dynamic weakening processes include frictional melting (Sibson, 1975; Di Toro et al., 2006), superplasticity (De Paola et al., 2015), and asperity flash heating (AFH), or transient, localized temperature pulses at asperity contacts (Archard, 1959; Lachenbruch, 1986; Rice, 2006). Minimum AFH temperatures are commonly inferred from textures and reaction products on exhumed and experimentally generated faults (Kohli et al., 2011; Proctor et al., 2014; Kuo et al., 2016; McDermott et al., 2017). Mapping the spatial distribution of, and quantifying, AFH temperatures can document earthquakes in the rock record and inform on the in situ mechanics and energy budget of earthquake rupture (Aubry et al., 2018; Hayward et al., 2019).

(U-Th)/He thermochronometry potentially serves as a fault slip thermometer (e.g., McDermott et al., 2017). This is because He diffusion kinetics of minerals on slip surfaces respond to short-duration, high-temperature thermal pulses (Reiners, 2009; Ault et al., 2015). Hematite, a common phase in fault zones, is amenable to (U-Th)/He thermochronometry (e.g., Wernicke and Lippolt, 1993; Farley and Flowers, 2012; Calzolari et al., 2018). Polycrystalline hematite typical of fault surfaces exhibits polydomain diffusion and a grain size–dependent closure temperature (T_c) from ~50–250 °C for a 10 °C/m.y. cooling rate (Evenson et al., 2014; Farley, 2018; Jensen et al., 2018). Recent work suggests that AFH can induce He loss in natural hematite fault mirrors (FMs)—thin (<1 mm), light-reflective, high-gloss slip surfaces—by temperature-induced recrystallization and/or volume diffusion (Ault et al., 2015; McDermott et al., 2017).

Here, we test the hypothesis that hematite He thermochronometry detects transient, cryptic thermal signatures of seismic slip on exhumed faults using frictional sliding experiments on specular hematite at seismic slip rates. We apply microtextural analysis and He thermochronometry of pre- and post-slip hematite to quantify frictional evolution, microstructural changes, and temperature-induced He loss. Analyses reveal that experimentally produced faults have FM zones analogous to those observed in natural fault rocks, with associated He-loss signatures consistent with AFH.

MATERIALS AND METHODS

Deformation experiments were performed on slabs created from a specular hematite boulder, collected from the central Wellsville Mountains, northeastern Utah (USA). Details of sample preparation and characterization, experimental setup, and post-run sampling are outlined in the GSA Data Repository[1]. Briefly, we acquired scanning electron microscopy (SEM) images of representative polycrystalline and single plates of hematite to characterize starting-material

[1]GSA Data Repository item 2020148, method details for SEM; grain-size measurement and distribution analysis and corresponding closure-temperature calculations; deformation experiment setup and sample preparation; (U-Th)/He sample preparation and analysis; temperature-rise and hematite He-loss calculations; and five data tables and 10 additional SEM, hematite He data, and calculation figures, is available online at http://www.geosociety.org/datarepository/2020/, or on request from editing@geosociety.org.

CITATION: Calzolari, G., et al., 2020, Hematite (U-Th)/He thermochronometry detects asperity flash heating during laboratory earthquakes: Geology, v. 48, p. 514–518, https://doi.org/10.1130/G46965.1

texture and grain size (i.e., hematite plate thickness). Plate thickness was measured with ImageJ software (https://imagej.net). Corresponding hematite He T_c was calculated assuming (1) correspondence of observable plate half-width to diffusion-domain length scale (Jensen et al., 2018), (2) hematite He diffusion kinetics of Farley (2018), and (3) a 10 °C/m.y. cooling rate. Material from the edge of each undeformed hematite slab was extracted and homogenized to create a uniform grain-size population to minimize grain-size effects on undeformed hematite He dates. These data serve as a benchmark for hematite He loss during deformation (see the Data Repository for sample preparation).

We used an Instron 1 atm rotary-shear apparatus at Brown University (Providence, Rhode Island, USA) to perform frictional-sliding experiments at ambient temperature and humidity and 8.5 MPa normal stress; the same apparatus was employed by Goldsby and Tullis (2011) and Kohli et al. (2011). The experimental setup involves a 4.77-mm-wide silicon carbide (SiC) ring (22.2 mm inner radius) sliding on a slab of specular hematite (Fig. DR1 in the Data Repository). Displacement per cycle is 36.5 mm (86° rotation), and cyclic inversion of slip direction yields higher total displacement. Data (torque, normal force, normal displacement, and angular displacement) are cataloged in the Data Repository (Figs. DR2–DR4).

We conducted two types of experiments to assess different aspects of He loss during fault slip. "Continuous slip" experiments comprised 40 cycles at the maximum slip velocity (~320 mm/s), with no interruptions between cycles, to produce the maximum frictional heat over 1500 mm total displacement. "Interrupted slip" experiments were conducted to the same total displacement, but comprised 40 cycles of: 2-mm-displacement at 0.01 mm/s, velocity step to ~320 mm/s for ~34 mm, and a 2-min "hold" before the next cycle.

Experimental fault surfaces were imaged with optical microscopy and SEM to characterize deformation textures and identify targets for hematite He analysis. Aliquots of undeformed and deformed material were analyzed for He, U, and Th to quantify He loss at the University of Arizona Radiogenic Helium Dating Laboratory (Tucson, Arizona, USA) using standard apatite lasing temperatures to prevent U and Th volatilization and modified zircon dissolution procedures (see the Data Repository for analytical details).

RESULTS

Undeformed Material

The starting material is polycrystalline, comprising randomly oriented hematite plates (i.e., individual grains; Fig. DR5). Plate thicknesses are 1–198 µm with a 17 ± 20 µm mean, corresponding to a T_c range of 114–197 °C and mean of 147 ± 13 °C (Fig. 1; Table DR1 in the Data Repository). Individual hematite He dates from 16 single plates spanning 75% of the observed plate thicknesses are 166 ± 11 Ma to 286 ± 10 Ma (±2σ analytical uncertainty). Dates exhibit a positive relationship with plate thickness and the corresponding calculated T_c (Fig. 1). Analyses (n = 2; Table DR2) with high Th/U and/or low U (see the Data Repository) are excluded from further discussion. Mean dates of homogenized material from each undeformed hematite slab are 211 ± 34 Ma for the continuous slip experiment (n = 3) and 177 ± 17 Ma for the interrupted slip experiment (n = 3) (±1σ standard deviation), which overlap with the range of single-plate hematite He dates (Fig. 1; Table DR2).

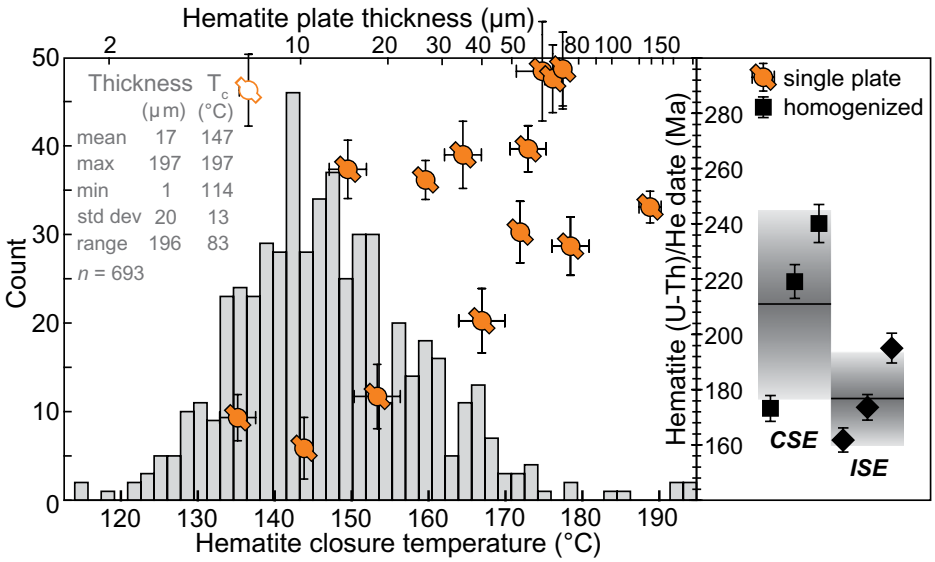

Figure 1. (Left panel) Single-plate hematite (U-Th)/He (hematite He) dates (orange symbols, 2σ error) versus plate thickness and closure temperature (T_c) (1σ error). Also shown is T_c calculated assuming Farley (2018) diffusion kinetics (gray histogram). White-filled symbol indicates data omitted from discussion (see the Data Repository [see footnote 1]). max—maximum; min—minimum; std dev—standard deviation. (Right panel) Undeformed homogenized hematite He dates (black symbols, 2σ error) with mean sample date (black line) and 1σ standard deviation (gray swath) for continuous and interrupted slip experiments (CSE and ISE, respectively).

Deformation Products

Friction data from continuous and interrupted slip experiments reveal that hematite has a low coefficient of friction (µ) of 0.28 ± 0.12 over a range of slip velocities (0.1–320 mm/s) and displacements (Figs. DR2–DR4), comparable to other platy minerals (e.g., Moore and Lockner, 2007). Interrupted slip experiments show a drop in µ in response to the velocity step. The friction drop (Δµ) is ~0.02 during the first cycle, and steadily increases to 0.12 over the course of the experiment, indicating evolution of the dynamic weakening behavior.

Both experiments yielded rust-colored hematite fault gouge on the hematite plate and SiC ring (Fig. 2; Fig. DR6). Gouge forms a continuous ~5–30 µm-thick layer with a sharp contact with undeformed hematite; an ~5-µm-thick gouge layer is observed on the SiC ring. Angular to subangular gouge particles are ~50 nm to 2 µm in diameter. Fault surfaces exhibit elongate (0.1–3-mm-wide, 0.3–6.5-mm-long), black, high-gloss FM zones on both hematite and SiC (Figs. 2A, 2B and 2I; Fig. DR6). FM zones make up >10% of continuous slip and <5% of interrupted slip surfaces by area. They are discontinuous on both surfaces, macroscopically striated, and pitted with gouge inclusions. In SEM, FM zones are ~10 µm thick and comprise flat, featureless layers of rounded 10–50-nm-diameter particles and sintered nanoparticle aggregates 70–800 nm in diameter (Fig. 2). Collectively, observations indicate that the fault surface developed within hematite gouge, closer to the SiC ring (Fig. 2I).

We report hematite He dates from FM zones and gouge generated during both experiments (Fig. 3; Table DR2). The number of analyses was limited by the material's delicate nature and our ability to exclusively isolate target textures in an aliquot. For the continuous slip experiment, three gouge aliquots (22G_H1–22G_H3) yield hematite He dates of 180 ± 3 Ma, 170 ± 3 Ma, and 169 ± 3 Ma (±2σ analytical uncertainty). Two FM aliquots (22S_H1, 22S_H3) yield dates of 62 ± 1 Ma and 59 ± 1 Ma. A third FM aliquot with an older 116 ± 2 Ma date has a high Th/U ratio, consistent with U volatilization during degassing, and is not considered in our discussion (Fig. DR8). For interrupted slip experiments, three gouge aliquots (23G_H1–23G_H3) yield dates of 137 ± 2 Ma, 157 ± 3 Ma, and 165 ± 3 Ma, and two FM aliquots (23S_H1, 23S_H2) yield dates of 113 ± 2 Ma and 117 ± 2 Ma. A third

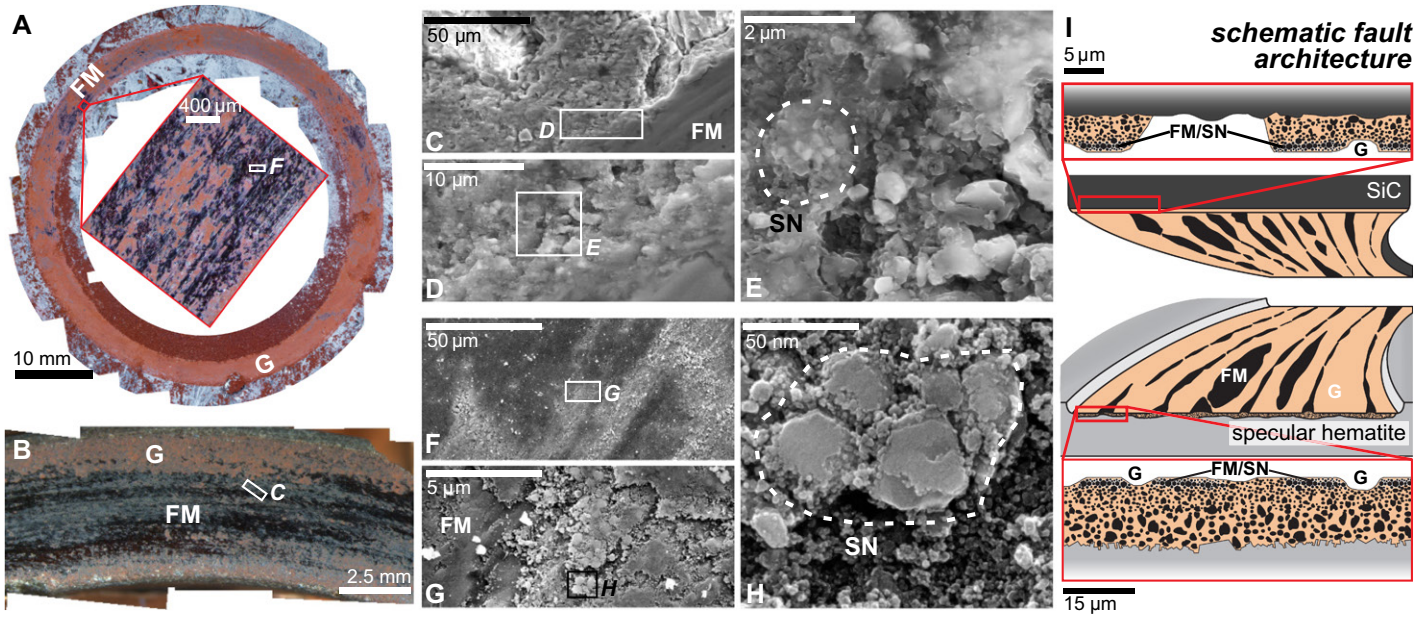

Figure 2. (A,B) Experimental fault-surface photo from hematite slab (A) and silicon carbide (SiC) ring (B) of the continuous slip experiment; inset zoom-in photo of fault mirror (FM) surface in A. G—gouge. (C–H) Scanning electron microscope images of FM for SiC (C–E) and hematite (F–H). SN—sintered nanoparticles. (I) Hematite fault architecture schematic.

FM aliquot with an 86 ± 1 Ma date has an elevated Th/U ratio and is not considered further (see the Data Repository; Fig. DR8). Thus, FMs exhibit the youngest dates in each experiment, continuous-slip FM dates are younger than interrupted-slip FM dates, and gouge dates overlap at 2σ with corresponding undeformed, homogenized hematite He dates from each experiment (Fig. 3).

COSEISMIC TEMPERATURE-INDUCED He LOSS

Younger hematite He dates from experimental FMs require faulting-induced He loss. To quantify He loss, we use a first-order approximation of the (U-Th)/He age (t) equation (Equation DR1 in the Data Repository) where t is proportional to [^{4}He]. We compare mean dates of undeformed homogenized material with FM and gouge hematite He dates from each experiment (see Table DR3 for full calculations). For continuous slip, He loss from FM and gouge is 71% ± 1% and 18% ± 3% (mean ± 1σ), respectively. He loss from interrupted-slip FM and gouge is 35% ± 2% and 13% ± 8% (Fig. 3). Thus, He loss occurs dominantly in FMs, and continuous-slip FMs exhibit ~50% more loss than interrupted-slip FMs. Calculated He loss is likely a minimum because FMs are <10 µm thick and analyzed aliquots may include coarser-grained, more retentive non-FM material. Continuous-slip gouge exhibits greater calculated He loss than interrupted-slip gouge, although He loss from both is minor. These calculations indicate coseismic frictional heating is the primary process responsible for the observed He loss.

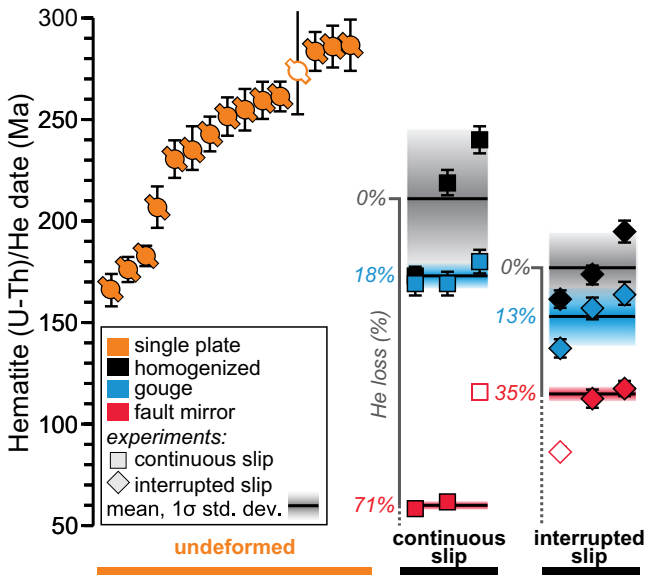

Figure 3. Individual hematite (U-Th)/He dates with 2σ analytical error from undeformed single plates and for homogenized hematite, gouge, and fault mirror aliquots from continuous and interrupted slip experiments, with calculated percent He loss. std. dev.—standard deviation. White-filled symbols indicate data omitted from discussion (see the Data Repository [see footnote 1]).

The temperatures and frictional-heating processes operative during slip can be estimated through analysis of (1) average fault-surface temperature rise and (2) AFH (Equations DR3 and DR4, respectively; Fig. 4). Both calculations consider the temperature for the maximum continuous displacement, which equates to 40 cycles for continuous slip and one cycle for interrupted slip experiments. Following Proctor et al. (2014), AFH calculations incorporate temperatures estimated through analysis of average fault-surface temperature rise.

We compare calculated fault thermal histories with calculated fractional He loss for FM aliquots (McDougall and Harrison, 1999; Reiners, 2009; Equation DR6). Fractional He loss curves in Figure 4 correspond to mean observed He loss, assume a square-pulse heating event, use He diffusion parameters of Farley (2018), and apply observed maximum and minimum hematite grain size in FM zones from each experiment (Fig. DR9). This comparison indicates that average fault-surface temperature rise alone—305 °C and 64 °C for continuous and interrupted slip experiments, respectively—does not explain observed He loss in FM zones (Fig. 4; Table DR5). FM He loss from both experiments is consistent with AFH at asperities >200–300 µm in diameter, capable of producing temperatures >900 °C for ~1 ms.

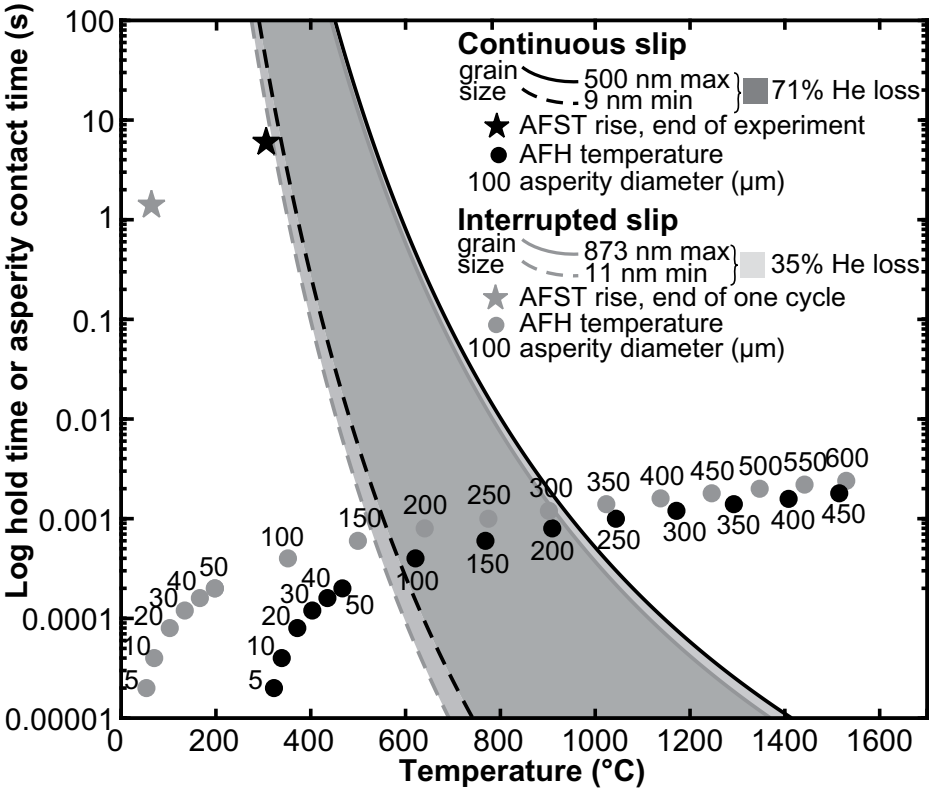

Figure 4. Calculated hematite He fractional loss contours for continuous (black curves) and interrupted (gray curves) slip experiments using maximum (max, solid line) and minimum (min, dashed line) grain sizes from fault mirror zones. Calculations assume square-pulse heating event and use He diffusion parameters from Farley (2018). Stars—peak average fault-surface temperature (AFST) at end of continuous slip experiment (black) and an interrupted slip cycle (gray); circles—peak asperity flash heating (AFH) temperatures calculated for different asperity diameters (in μm), assuming asperity lifetimes that scale with diameter, and maximum AFST in continuous (black) and interrupted (gray) slip experiments.

ASPERITY FLASH HEATING AND He LOSS MECHANISMS

Results support coseismic AFH causing the observed textural changes and He loss in FM zones. Comminution, which commonly occurs during seismic slip (Stünitz et al., 2010), decreases the diffusion-domain length scale, and in turn, decreases temperatures required to cause He loss during AFH (Fig. DR10; Ault et al., 2015). Our experimental FMs comprise sintered nanoparticles, texturally distinct from polygonal, recrystallized grains observed on other natural hematite fault mirrors (Ault et al., 2015, 2019; McDermott et al., 2017). We model He loss as thermally activated volume diffusion for simplicity, and note that the effects of sintering, a thermal process, on He loss are not known. Regardless, the spatial association between localized He loss and sintering suggests that both are related to AFH. In addition, average fault-surface temperature rise influences AFH-induced He loss (see Equation DR4) and may induce partial He loss from ultrafine gouge particles (Figs. 3 and 4; Fig. DR10). Compared to continuous-slip results, interrupted-slip data show a lower magnitude of FM and gouge He loss as well as a lower surface area of FM zones, implying that average fault-surface temperatures decrease between cycles in this experiment.

Interestingly, our inferred asperity size (>200–300 μm diameter; Fig. 4), assuming a typical asperity lifetime that scales with diameter, is larger than conventional theory (~10–50 μm; e.g., Rice, 2006). Smaller-diameter asperities with longer contact times can achieve the same temperatures. Assuming that experimentally generated FMs are trackways of paleoasperities, the high-aspect-ratio FMs (Figs. 2A and 2B) are an order-of-magnitude longer than expected, supporting an asperity ploughing process. Although textures, He loss, and calculated temperatures may reflect our experimental conditions, this study offers new empirical evidence of AFH conditions.

PINPOINTING EARTHQUAKES IN THE ROCK RECORD

Our experiments reveal that hematite He thermochronometry and other (U-Th)/He systems with similar diffusion kinetics can serve as paleotemperature proxies in fault rocks. These tools, when combined with textural analysis and constraints on the post-slip ambient thermal history (e.g., Ault et al., 2015; McDermott et al., 2017), can pinpoint past earthquakes in the uppermost crust in exhumed fault zones. Previously, minimum AFH temperatures were inferred to explain thermal decomposition in carbonates (Han et al., 2007; De Paola et al., 2011) and serpentine (Viti and Hirose, 2010; Kohli et al., 2011), as well as high-temperature iron reduction (Evans et al., 2014) on natural and experimental faults. Our work indicates that (U-Th)/He thermochronometry can map out the spatial distribution of AFH temperatures on fault surfaces to inform earthquake mechanics at the upper end of the seismogenic zone.

ACKNOWLEDGMENTS

We thank editor Mark Quigley, Rich Ketcham, and an anonymous reviewer for their feedback which improved our manuscript. This work was supported by National Science Foundation CAREER (1654628) and Southern California Earthquake Center (SCEC; 17164) grants to Ault. We thank Pete Reiners, FenAnn Shen, Uttam Chowdhury, Terry Tullis, and Chandrasekar Minnal for analytical assistance.

REFERENCES CITED

Archard, J.F., 1959, The temperature of rubbing surfaces: Wear, v. 2, p. 438–455, https://doi.org/10.1016/0043-1648(59)90159-0.

Aubry, J., Passelègue, F.X., Deldicque, D., Girault, F., Marty, S., Lahfid, A., Bhat, H.S., Escartin, J., and Schubnel, A., 2018, Frictional heating processes and energy budget during laboratory earthquakes: Geophysical Research Letters, v. 45, p. 12,274–12,282, https://doi.org/10.1029/2018GL079263.

Ault, A.K., Reiners, P.W., Evans, J.P., and Thomson, S.N., 2015, Linking hematite (U-Th)/He dating with the microtextural record of seismicity in the Wasatch fault damage zone, Utah, USA: Geology, v. 43, p. 771–774, https://doi.org/10.1130/G36897.1.

Ault, A.K., Jensen, J.L., McDermott, R.G., Shen, F.A., and Van Devener, B.R., 2019, Nanoscale evidence for temperature-induced transient rheology and postseismic fault healing: Geology, v. 47, p. 1203–1207, https//doi.org/10.1130/G46317.1.

Calzolari, G., Rossetti, F., Ault, A.K., Lucci, F., Olivetti, V., and Nozaem, R., 2018, Hematite (U-Th)/He thermochronometry constrains intraplate strike-slip faulting on the Kuh-e-Faghan Fault, central Iran: Tectonophysics, v. 728, p. 41–54, https://doi.org/10.1016/j.tecto.2018.01.023.

De Paola, N., Hirose, T., Mitchell, T., Di Toro, G., Viti, C., and Shimamoto, T., 2011, Fault lubrication and earthquake propagation in thermally unstable rocks: Geology, v. 39, p. 35–38, https://doi.org/10.1130/G31398.1.

De Paola, N., Holdsworth, R.E., Viti, C., Collettini, C., and Bullock, R., 2015, Can grain size sensitive flow lubricate faults during the initial stages of earthquake propagation?: Earth and Planetary Science Letters, v. 431, p. 48–58, https://doi.org/10.1016/j.epsl.2015.09.002.

Di Toro, G., Hirose, T., Nielsen, S., Pennacchioni, G., and Shimamoto, T., 2006, Natural and experimental evidence of melt lubrication of faults during earthquakes: Science, v. 311, p. 647–649, https://doi.org/10.1126/science.1121012.

Di Toro, G., Han, R., Hirose, T., De Paola, N., Nielsen, S., Mizoguchi, K., Ferri, F., Cocco, M., and Shimamoto, T., 2011, Fault lubrication during earthquakes: Nature, v. 471, p. 494–498, https://doi.org/10.1038/nature09838.

Evans, J.P., Prante, M.R., Janecke, S.U., Ault, A.K., and Newell, D.L., 2014, Hot faults: Iridescent slip surfaces with metallic luster document high-temperature ancient seismicity in the Wasatch fault zone, Utah, USA: Geology, v. 42, p. 623–626, https://doi.org/10.1130/G35617.1.

Evenson, N.S., Reiners, P.W., Spencer, J.E., and Shuster, D.L., 2014, Hematite and Mn oxide (U-Th)/He dates from the Buckskin-Rawhide detachment system, western Arizona: Gaining insights into hematite (U-Th)/He systematics: American Journal of Science, v. 314, p. 1373–1435, https://doi.org/10.2475/10.2014.01.

Farley, K.A., 2018, Helium diffusion parameters of hematite from a single-diffusion-domain crystal: Geochimica et Cosmochimica Acta, v. 231, p. 117–129, https://doi.org/10.1016/j.gca.2018.04.005.

Farley, K.A., and Flowers, R.M., 2012, (U-Th)/Ne and multidomain (U-Th)/He systematics of a hydrothermal hematite from eastern Grand Canyon: Earth and Planetary Science Letters, v. 359–360, p. 131–140, https://doi.org/10.1016/j.epsl.2012.10.010.

Goldsby, D.L., and Tullis, T.E., 2011, Flash heating leads to low frictional strength of crustal rocks at earthquake slip rates: Science, v. 334, p. 216–218, https://doi.org/10.1126/science.1207902.

Han, R., Shimamoto, T., Hirose, T., Ree, J.-H., and Ando, J.-i., 2007, Ultralow friction of carbonate faults caused by thermal decomposition: Science, v. 316, p. 878–881, https://doi.org/10.1126/science.1139763.

Hayward, K.S., Hawkins, R., Cox, S.F., and Le Losq, C., 2019, Rheological controls on asperity weakening during earthquake slip: Journal of Geophysical Research: Solid Earth, v. 124, p. 12,736–12,762, https://doi.org/10.1029/2019JB018231.

Jensen, J.L., Siddoway, C.S., Reiners, P.W., Ault, A.K., Thomson, S.N., and Steele-MacInnis, M., 2018, Single-crystal hematite (U-Th)/He dates and fluid inclusions document widespread Cryogenian sand injection in crystalline basement: Earth and Planetary Science Letters, v. 500, p. 145–155, https://doi.org/10.1016/j.epsl.2018.08.021.

Kanamori, H., and Riviera, L., 2006, Energy partitioning during an earthquake, *in* Abercrombie, R., et al., eds., Earthquakes: Radiated Energy and the Physics of Faulting: American Geophysical Union Geophysical Monograph 170, p. 3–13, https://doi.org/10.1029/170GM03.

Kohli, A.H., Goldsby, D.L., Hirth, G., and Tullis, T., 2011, Flash weakening of serpentinite at near-seismic slip rates: Journal of Geophysical Research, v. 116, B03202, https://doi.org/10.1029/2010JB007833.

Kuo, L.-W., Song, S.-R., Suppe, J., and Yeh, E.-C., 2016, Fault mirrors in seismically active fault zones: A fossil of small earthquakes at shallow depths: Geophysical Research Letters, v. 43, p. 1950–1959, https://doi.org/10.1002/2015GL066882.

Lachenbruch, A.H., 1986, Simple models for the estimation and measurement of frictional heating by an earthquake: U.S. Geological Survey Open-File Report 86-508, 13 p., https://doi.org/10.3133/ofr86508.

McDermott, R.G., Ault, A.K., Evans, J.P., and Reiners, P.W., 2017, Thermochronometric and textural evidence for seismicity via asperity flash heating on exhumed hematite fault mirrors, Wasatch fault zone, UT, USA: Earth and Planetary Science Letters, v. 471, p. 85–93, https://doi.org/10.1016/j.epsl.2017.04.020.

McDougall, I., and Harrison, T.M., 1999, Geochronology and Thermochronology by the $^{40}Ar/^{39}Ar$ Method (second edition): Oxford, UK, Oxford University Press, 288 p.

Moore, D.E., and Lockner, D.A., 2007, Friction of the smectite clay montmorillonite: A review and interpretation of data, *in* Dixon, T., and Moore, J.C., eds., The Seismogenic Zone of Subduction Thrust Faults: New York, Columbia University Press, p. 317–345, https://doi.org/10.7312/dixo13866-011.

Proctor, B.P., Mitchell, T.M., Hirth, G., Goldsby, D., Zorzi, F., Platt, J.D., and Di Toro, G., 2014, Dynamic weakening of serpentinite gouges and bare surfaces at seismic slip rates: Journal of Geophysical Research: Solid Earth, v. 119, p. 8107–8131, https://doi.org/10.1002/2014JB011057.

Reiners, P.W., 2009, Nonmonotonic thermal histories and contrasting kinetics of multiple thermochronometers: Geochimica et Cosmochimica Acta, v. 73, p. 3612–3629, https://doi.org/10.1016/j.gca.2009.03.038.

Rice, J.R., 2006, Heating and weakening of faults during earthquake slip: Journal of Geophysical Research, v. 111, B05311, https://doi.org/10.1029/2005JB004006.

Rowe, C.D., and Griffith, W.A., 2015, Do faults preserve a record of seismic slip: A second opinion: Journal of Structural Geology, v. 78, p. 1–26, https://doi.org/10.1016/j.jsg.2015.06.006.

Sibson, R.H., 1975, Generation of pseudotachylyte by ancient seismic faulting: Geophysical Journal International, v. 43, p. 775–794, https://doi.org/10.1111/j.1365-246X.1975.tb06195.x.

Stünitz, H., Keulen, N., Hirose, T., and Heilbronner, R., 2010, Grain size distribution and microstructures of experimentally sheared granitoid gouge at coseismic slip rates—Criteria to distinguish seismic and aseismic faults?: Journal of Structural Geology, v. 32, p. 59–69, https://doi.org/10.1016/j.jsg.2009.08.002.

Viti, C., and Hirose, T., 2010, Thermal decomposition of serpentine during coseismic faulting: Nanostructures and mineral reactions: Journal of Structural Geology, v. 32, p. 1476–1484, https://doi.org/10.1016/j.jsg.2010.09.009.

Wernicke, R.S., and Lippolt, H.J., 1993, Botryoidal hematite from the Schwarzwald (Germany): Heterogeneous uranium distributions and their bearing on the helium dating method: Earth and Planetary Science Letters, v. 114, p. 287–300, https://doi.org/10.1016/0012-821X(93)90031-4.

Printed in USA